



Title	Versatile Simple Doping Technique for Diamond by Solid Dopant Source Immersion during Microwave Plasma CVD
Author(s)	Tamura, Takahiro; Yanase, Takashi; Nagahama, Taro; Wakeshima, Makoto; Hinatsu, Yukio; Shimada, Toshihiro
Citation	Chemistry Letters, 43(10), 1569-1571 <a href="https://doi.org/10.1246/cl.140598">https://doi.org/10.1246/cl.140598</a>
Issue Date	2014-10-05
Doc URL	<a href="http://hdl.handle.net/2115/57577">http://hdl.handle.net/2115/57577</a>
Type	article (author version)
File Information	tamura1_CL_HUSCAP.pdf



[Instructions for use](#)

**Versatile simple doping technique for diamond**  
**by solid dopant source immersion during microwave plasma CVD**

Takahiro Tamura<sup>1</sup>, Takashi Yanase<sup>2</sup>, Taro Nagahama<sup>3</sup>, Makoto Wakeshima<sup>4</sup>, Yukio Hinatsu<sup>4</sup>, Toshihiro Shimada<sup>3\*</sup>

<sup>1</sup>*Graduate School of Chemical Science and Engineering, Hokkaido University, Kita-ku, Sapporo, 060-8628, Japan*

<sup>2</sup>*Frontier Chemistry Center, Hokkaido University, Kita-ku, Sapporo, 060-8628, Japan*

<sup>3</sup>*Division of Materials Chemistry, Faculty of Engineering, Hokkaido University, Kita-ku, Sapporo, 060-8628, Japan*

<sup>4</sup>*Department of Chemistry, Faculty of Science, Hokkaido University, Kita-ku, Sapporo, 060-0810, Japan*

(Received <Month> <Date>, <Year>; CL-<No>; E-mail: <insert corresponding e-mail address>)

We demonstrate a new doping technique for CVD growth of diamond. The method involves immersing a solid state dopant source into the plasma of microwave plasma-assisted CVD. We applied this simple and versatile technique to the growth of boron-doped diamond. The grown films were characterized by X-ray diffraction (XRD), Raman spectroscopy, glow discharge optical emission spectroscopy (GDOES) and electrical conductivity measurement. The average concentration of boron was 0.5 atomic % and the conductivity was  $1.5 \times 10^{-2} \Omega\text{cm}$ , which showed irregular behavior at low temperature.

The variety of thin film materials and devices is continuously increasing because of incessant development of their deposition techniques<sup>1</sup>. It has become possible to control the nano-scale integration of various materials including semiconductors, metals, oxides, organic molecular materials and polymers<sup>2-6</sup>, which has enabled high performance and light-weight devices with new functions and yet saving resources.

Various novel thin film devices using doped diamonds have emerged recently, which include highly B-doped diamonds showing superconductivity<sup>7,8</sup>, deep-UV LED fabricated from diamond p-n junctions<sup>9</sup>, single photon sources realized by isolated NV centers in diamonds<sup>10</sup>. These unique functions of the devices originate mainly from the wide band gap and the ultra-hard lattice of diamonds, which create distinctive dopant states. Theoretical investigations predict that there are plenty of novel doped diamonds that have never been synthesized, such as n-type diamonds by co-doping of multiple elements<sup>11,12</sup>. Despite the long history of the doped diamonds<sup>13</sup>, it is worth pursuing the synthesis of novel doped diamonds.

Three methods are commonly used to fabricate doped diamonds: CVD growth with gas-phase dopants, dopant ion implantation to a diamond crystal and a spray mist supply of dopant solution. It is difficult to explore the full possibility of doped diamonds by these methods because of their many limitations. Although the doping of light elements such as B, N and P is possible by introducing gas phase dopants ((CH<sub>3</sub>)<sub>3</sub>B, NH<sub>3</sub>, and PH<sub>3</sub>, respectively) during plasma CVD, the handling of these dopant gases is difficult and costly due to their very toxic and flammable nature. There are many elements that do not have volatile compounds from the beginning. The ion implantation is a more versatile technique, but it requires annealing to settle the interstitial dopant atoms in the crystal lattice. The material approaches thermal equilibrium by annealing, which expels the dopants above a certain concentration. This diminishes the flexibility of the dopant choice and the maximum concentration. The ion implantation also has a drawback of inhomogeneous doping in the depth direction. The spray mist supply of dopants is used only for boron doping in the literature<sup>14</sup>. It is very convenient but might have problems of impurity or aggregation of the dopants.

In order to remove these limitations, we attempted doping of diamond using solid sources, i.e., by immersing a polycrystalline boron rod into the H<sub>2</sub> - CH<sub>4</sub> plasma during the microwave plasma chemical vapor deposition (MPCVD) of the diamonds. This method is free from the limitations of the currently used techniques because it does not use gaseous dopants nor require annealing. The grown films were characterized by X-ray diffraction (XRD), Raman spectroscopy, glow discharge optical emission spectroscopy (GDOES) and electrical conductivity measurement.

We used a center - antenna type MPCVD equipment (Arios Inc., DCVD-51A) for the growth of diamond thin films. Microwave energy (2.45 GHz) from a solid state power supply was emitted from the antenna rod sticking out at the center of a spherical chamber. The microwave energy is reflected by the inner wall of the spherical chamber made of stainless steel and resonates. The sample holder ( $\phi$  10 mm molybdenum) was placed on the antenna rod. The microwave power was concentrated at the sample holder and plasma was ignited in H<sub>2</sub> - CH<sub>4</sub> atmosphere. The intense plasma was limited within a spherical area of 15-mm diameter, which enables diamond synthesis at low power (~ 200 W). This equipment also has the merit of low contamination because the plasma does not touch the chamber wall. We modified the equipment by attaching a linear motion to insert a boron rod ( $\phi$  6 mm  $\times$  L 30 mm) along the direction 45° off from the sample normal (Fig. 1).

The electrostatic potential of the boron rod and the sample holder can be modified separately up to  $\pm 500$  V from the chamber wall. The temperature was monitored by a radiation thermometer (Minolta TR-630A, using the emissivity 0.75 for Si and 0.95 for diamond).

In the diamond growth experiment, we used substrates of high resistivity Si(100) wafer (cut into 5mm - 10 mm square) and diamond (100) single crystals (2.5 x 2.5 x 0.2 mm). The Si wafers were cleaned by the RCA method to remove contamination. The diamond (100) crystals were cleaned by H<sub>2</sub> gas plasma at 1000 °C with 6 kPa H<sub>2</sub> discharged by 200W microwave energy for 6 h to remove sp<sup>2</sup> components. In order to grow thin diamond films on Si, the nucleation was enhanced by applying a static bias<sup>15</sup> (-300 V) to the sample in the beginning 30 minutes of MPCVD in CH<sub>4</sub> : H<sub>2</sub> = 6% : 94% and a total pressure of 3 kPa. This procedure was omitted for the growth on diamond (001) surfaces.

The growth condition of the B-doped diamond was optimized to obtain the largest crystalline grains as follows: CH<sub>4</sub> : H<sub>2</sub> = 1.2% : 98.8%, total pressure was 6 kPa, the surface temperature was 1000 °C, and the surface cleaning and the nucleation procedure were as stated above. The boron rod, penetrating into the plasma along the direction 45° off from the surface normal, was placed at 15 mm from the sample surface. This distance is an optimized one for the uniformity of the plasma and maximum doping concentration. Figure 2 shows the optical image of the sample and the boron rod during the MPCVD growth. The growth was continued for 24 h. We applied + 450 V against the chamber wall to both the sample holder and the boron rod in order to avoid carbon contamination of the boron surface and enhance the growth of the diamond. Without applying the positive bias to the boron rod, the surface of the rod becomes dusty due to the growth of carbon species.

Figure 3 shows the laser optical microscope images (Keyence VK-8710) of the boron doped diamond on Si(001) and diamond (001). Microcrystalline films with 10- to 50-  $\mu\text{m}$  crystal grains were obtained on both substrates. XRD was obtained from the sample grown on Si(001) to examine the crystallinity of the film (Fig. 4). It was confirmed that diamond crystals were grown without graphite or other carbon allotropes.

We next characterized the sample grown on Si(100) by Raman microscopy (Renishaw InVia with 532- nm excitation). It is reported that Raman peak shapes are strongly dependent on the boron concentration<sup>16,17</sup> and that they can be used to estimate the boron concentration. The Raman spectra differed considerably from position to position on the 10 x 10 mm sample. The measured areas were 2-  $\mu\text{m}$  spots in 10 ~ 20 $\mu\text{m}$  crystalline grains. The center position exhibited two peaks at 480  $\text{cm}^{-1}$  and 1250  $\text{cm}^{-1}$  (Fig. 5(a)) that are characteristic of boron-doped diamond (111). By comparing the spectrum shapes with those in the literature<sup>16,17</sup>, the boron concentration at this position was estimated to be 1 %.

The boron concentrations at the sample edge (Fig. 5(b)) and the sample corner (Fig. 5(c)) were estimated to be 0.5 % and 0.02%, respectively. The distribution of the boron concentration is almost concentric, although the boron rod was immersed unsymmetrically relative to the sample normal. This is because the distance between the boron rod and the sample surface was regulated so as not to disturb the spherical symmetry of the plasma. Therefore, the reason for this inhomogeneity of the boron concentration is related to the fact that the growth speed is faster near the periphery of the samples.

We measured the boron concentration in the diamond by GDOES (Horiba Jobin Yvon GD-Profiler). This method quantifies the intensity of element-specific optical emission of sputtered atoms by Ar glow discharge. We used a sintered polycrystalline  $\text{B}_4\text{C}$  disc as the standard material to derive the B/C ratio in the diamond. B : C = 0.5% : 99.5%. Because the GDOES measures the whole sample (4mm  $\phi$ ) as average, this result agrees well with the Raman results.

In order to study the electronic properties of the boron-doped diamond films, we measured the electrical conductivity at low temperature. We attached four electrodes on a 6- mm square sample grown on highly resistive Si(001) and measured the conductivity down to 1.8 K (Quantum Design PPMS). The thickness of the B-doped diamond film was 10  $\mu\text{m}$  with a 20-  $\mu\text{m}$  buffer (and insulation) layer of undoped diamond. Note that the sample contained regions of various B concentrations as shown in Fig. 5. We measured many samples and the result showing the lowest resistivity at low temperature is shown in Fig. 6. It shows relatively low resistivity around  $1.5 \times 10^{-2} \Omega\text{cm}$ . This value is low enough for electrochemical applications<sup>18,19</sup>. The resistivity increased when the temperature decreased from 300 K to 60 K but decreased when the temperature decreased below 60K. This strange behavior, including steep decrease below 2.5 K, seems to arise from the inhomogeneity of the boron concentration in the film. Attempt to prepare smaller samples for the better uniformity to observe the superconductive zero-resistivity was not successful so far.

In summary, we have developed a new technique to grow thin doped diamond films. The method involves simply immersing the solid dopant source into the plasma of microwave plasma CVD to sputter and atomize the dopant elements. We demonstrated the doping of boron from a sintered boron rod and characterized the sample by x-ray diffraction, Raman spectroscopy and GDOES. We found that 1% B-doping is possible but the concentration of boron is rather inhomogeneous, distributing 1% to 0.02% within a 10- mm sample. This technique is suitable for examining the possibility of doping of various elements including multiple dopants.

This work was partly supported by CREST-JST (Project leader : Prof. T. Hasegawa, The University of Tokyo).

## References

- 1 K. Ariga, Y. Yamauchi, G. Rydzek, Q. Ji, Y. Yonamine, K. C.-W. Wu, and J. P. Hill, *Chem. Lett.* **2014**, *43*, 36.
- 2 K. Togashi, Y. Sagara, T. Yasuda, C. Adachi, *Chem. Lett.* **2013**, *42*, 651.
- 3 Y. Muronoi, J. Zhang, M. Higuchi, H. Maki, *Chem. Lett.* **2013**, *42*, 761.
- 4 M. Kawasaki, *Bull. Chem. Soc. Jpn.* **2013**, *86*, 1341.
- 5 Y. Shimakawa, *Bull. Chem. Soc. Jpn.* **2013**, *86*, 299.
- 6 Y. Matuso, *Chem. Lett.* **2012**, *41*, 754.
- 7 Y. Takano, M. Nagao, I. Sakaguchi, M. Tachiki, T. Hatano, K. Kobayashi, H. Umezawa, H. Kawarada, *Appl. Phys. Lett.* **2004**, *85*, 2851.
- 8 T. Muranaka, K. Kobashi, H. Okabe, T. Tachibana, Y. Yokota, K. Hayashi, N. Kawakami, J. Akimitsu, *Diamond & Related Materials* **2011**, *20*, 123.
- 9 S. Koizumi, K. Watanabe, M. Hasegawa, H. Kanda, *Science* **2001**, *292*, 1899.
- 10 N. Mizuochi, T. Makino, H. Kato, D. Takeuchi, M. Ogura, H. Okushi, M. Nothhaft, P. Neumann, A. Gali, F. Jelezko, J. Wrachtrup, S. Yamasaki, *Nature Photonics* **2012**, *6*, 299.
- 11 U. Schwingenschlögl, A. Chroneos, C. Schuster, R. W. Grimes, *J. Appl. Phys.* **2011**, *110*, 056107.
- 12 R. J. Eyre, J. P. Goss, P. R. Briddon, M. G. Wardle, *Phys. Stat. Sol. (a)* **2007**, *204*, 2971.
- 13 R. Kalish, *Carbon* **1999**, *37*, 781.
- 14 T. Yano, D.A. Tryk, K. Hashimoto, A. Fujishima, *J. Electrochem. Soc.* **1998**, *145*, 1870.
- 15 S. Yugo, T. Kanai, T. Kimura, T. Muto, *Appl. Phys. Lett.* **1991**, *58*, 1036.
- 16 R.J. Zhang, S.T. Lee, Y.W. Lam, *Diamond and Related Materials* **1996**, *5*, 1288.
- 17 T. Watanabe, T. K. Shimizu, Y. Tateyama, Y. Kim, M. Kawai, Y. Einaga, *Diamond and Related Materials* **2010**, *19*, 772.
- 18 A. Suzuki, T.A. Ivandini, K. Yoshimi, A. Fujishima, G. Oyama, T. Nakazato, T. N.Hattori, S. Kitazawa, Y. Einaga, *Anal. Chem.* **2007**, *79*, 8608.
- 19 K. Nakata, T. Ozaki, C. Terashima, A. Fujishima, Y. Einaga, *Angew. Chem. Int'l Ed.* **2014**, *53*, 871.

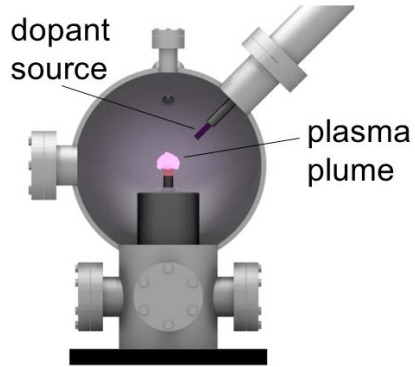


**Figure 1.** Cross sectional drawing of MPCDV chamber with solid state dopant.



**Figure 2.** Optical image of the sample and the boron rod.

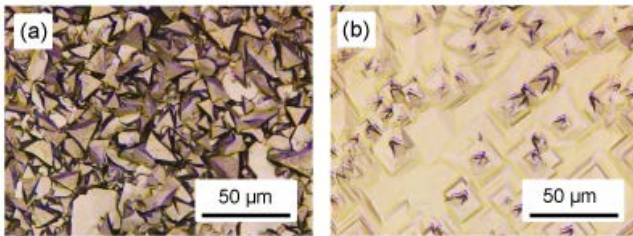


**Figure 3.** Laser microscope images of diamond film grown on (a) Si(001) and (b) diamond (001).

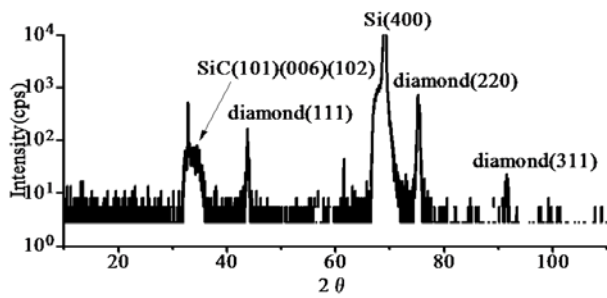


**Figure 4.** X-ray diffraction of boron-doped diamond grown on Si(001).

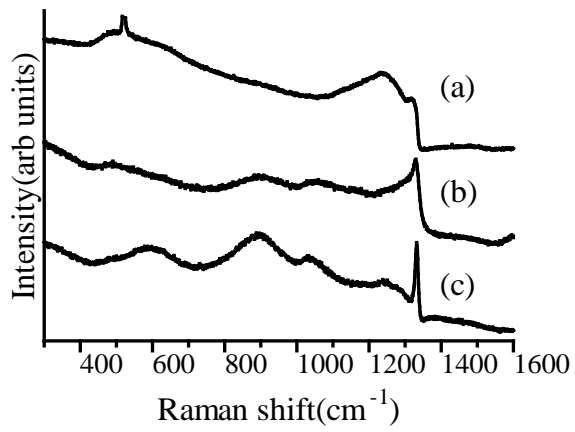


**Figure 5.** Raman spectra of a boron-doped diamond at different positions. (a) center (b) edge (c) corner.

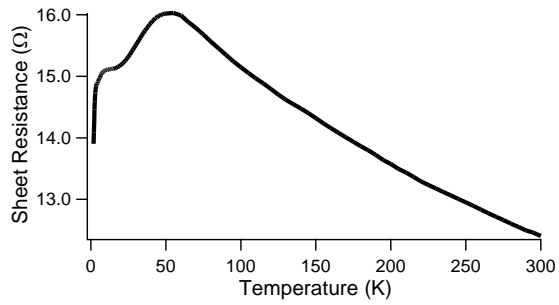


**Figure 6.** Sheet resistance of a boron-doped diamond film (thickness 10  $\mu\text{m}$ ) grown on an undoped diamond buffer layer (thickness 20  $\mu\text{m}$ ) on Si(001).